

Review Paper

Fabrication of Stretchable Transparent Electrodes

Jong Sik Oh^a and Geun Young Yeom^{a,b*}

^a*School of Advanced Materials Science and Engineering, Sungkyunkwan University, 2066 Seobu-ro, Jangan-gu, Suwon-si, Gyeonggi-do 16419, Republic of Korea*

^b*SKKU Advanced Institute of Nano Technology (SAINT), Sungkyunkwan University, 2066 Seobu-ro, Jangan-gu, Suwon-si, Gyeonggi-do 16419, Republic of Korea*

Received July 18, 2017; revised October 22, 2017; accepted October 23, 2017

Abstract Recently, stretchable and transparent electrodes have received great attention owing to their potential for realizing wearable electronics. Unlike the traditional transparent electrodes represented by indium tin oxide (ITO), stretchable and transparent electrodes are able to maintain their electrical and mechanical properties even under stretching stress. Lots of research efforts have been dedicated to the development of stretchable and transparent electrodes since they represent the most important engineering platform for the production of wearable electronics. Various approaches using silver nanowires, nanostructured networks, conductive polymers, and carbon-based electrodes have been explored by many world leading research groups. In this review, present and recent advances in the fabrication methods of stretchable and transparent electrodes are discussed.

Keywords: Transparent electrode, Stretchable electrode, Wearable

I. Introduction

Wearable electronics are rapidly evolving towards a new generation of deformable electronics, i.e., electronic devices that can be flexible, rollable, and stretchable.¹⁻⁷ Especially, stretchable electronics represent one of the most sophisticated and complicated technologies, since each of their constituting components must not only overcome the compressive and tensile stress, but also maintain its electrical and mechanical properties during stretching in various directions [8-9]. Therefore, many researchers have explored the development of deformable materials that can replace the elements constituting the conventional electronic devices. For all electronic devices fabricated on rigid substrates, such as flat panel displays, touch panels, solar cells, and smart windows, indium tin oxide (ITO) has been adopted as transparent electrode owing to its excellent electrical and optical properties. However, with the advent of evolutionary technologies allowing the realization of deformable electronics on stretchable substrates, it has become necessary to search for other transparent electrode materials that can replace ITO, since it can significantly lose its electrical and mechanical properties upon stretching, bending, or rolling [10-11]. Furthermore, due to the limited global reserves of ITO and consequential price fluctuations depending on demand and supply, its manufacturing cost is

continuously increasing [10,12].

In this context, we wish to focus our discussion on the principal fabrication methods and current issues of next generation stretchable transparent electrode materials. Beyond the use of conventional ITO, in the past several years many research groups have increasingly explored the viability of stretchable transparent electrodes such as silver nanowires (AgNWs), nanostructured networks, conductive polymers, carbon-based electrodes, and nanotrough networks, which in some cases exhibited outstanding flexibility, electrical and optical properties.

II. Fabrication Methods

1. Silver nanowires (AgNWs)

Various growth methods for the preparation of single crystalline metallic nanowires have been developed by many research groups, since they represent the most promising next generation transparent electrode materials. Among the several metallic nanowires that have been produced so far from copper, gold, and silver, AgNWs have raised particular interest since they exhibit outstanding electrical and optical properties compared with the other metallic nanowires due to their synthetic scalability that allows to obtain extremely thin and long materials [13-17]. Therefore, in this review, we summarize some of the latest fabrication processes of stretchable transparent electrodes made of AgNWs.

In order to achieve a stretchable conductive AgNW

*Corresponding author
E-mail: gyeom@skku.edu

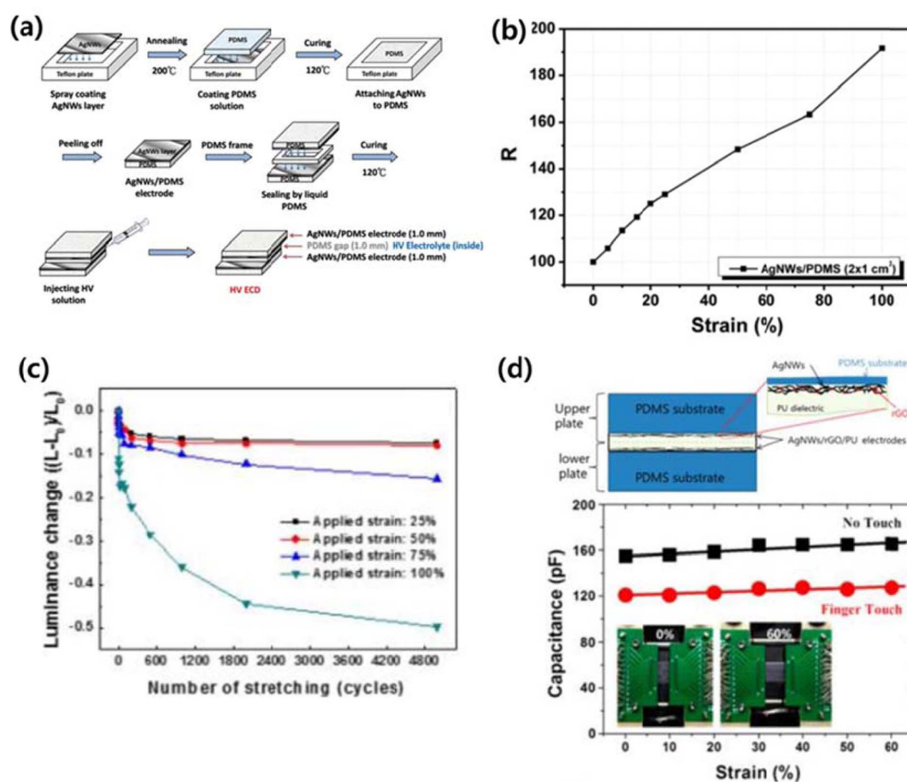


Figure 1(a) Schematic diagram of the fabrication of AgNW/PDMS hybrid electrodes and elastomeric HV ECDs (b) The resistance variation of the AgNW/PDMS hybrid electrode for stretching test. (a) and (b) Reprinted with permission from [21], Liou et al., *Nanoscale* 9, 7 (2017). © 2017, Royal Society of Chemistry. (c) Number of stretch-release tests under various applied strain values. Reprinted with permission from [7], J. W. Kim et al., *ACS Appl Mater Inter* 9, 21 (2017). © 2017 American Chemical Society. (d) Schematic of transparent and stretchable capacitive sensor and the capacitance change in single capacitive touch sensor under stretching strain with (red) and without (black) touching (inset: photographs of single capacitive touch sensor with 0% (left) and 60% (right) of stretching during stretching test). Reprinted with permission from [20], N. E. Lee et al., *ACS Appl Mater Inter* 9, 21 (2017). © 2017 American Chemical Society.

electrode embedded within a stretchable polymer such as polyurethane (PU), poly(styrene-block-butadiene-block-styrene) (SBS), polystyrene-polyisoprene-polystyrene (SIS), and poly(dimethylsiloxane) (PDMS), common liquid coating methods including spray, spin, and dip coating processes cannot be employed owing to a weak junction cohesion that may lead to a loss of electrical conductivity under the stretching strain [7,18-29]. In order to preserve the electrical properties of AgNWs, while overcoming the crucial issues mentioned above, many research groups have proposed hybrid AgNW structures to fabricate stretchable transparent electrodes.

Figure 1 shows the hybrid structures obtained by combining AgNWs with PDMS. The most common process to fabricate hybrid AgNW/PDMS electrodes is an embedding process that was developed by Liou et al. [21]; the schematic diagram of this process is depicted in Figure 1a. Firstly, an AgNW/ethanol solution was spray-coated on the detachable substrate by using an airbrush gun, and subsequently the above PDMS viscous liquid was poured onto a substrate. After curing, the AgNW/PDMS hybrid film was peeled off from the substrate. In the case of G. S. Liou et al., a syringe was used to inject a solution of heptyl viologen (HV) with an electrolyte (0.005 M in CH₃CN

containing 0.1 M TBAP as supporting electrolyte) between two hybrid AgNW/PDMS electrodes to fabricate electrochromic devices (ECDs). However, despite the advantage of the easy fabrication of a stretchable transparent electrode, it was observed that the resistance increased linearly as the stretch strain increased, as shown in Figure 1b. This is because the stretch strain produces a significant stress at the junction of AgNWs and reduces conductivity due to the weak contact adhesion between the wires.

In other reports by Kim et al. and Lee et al., polyurethane urea (PUU) or reduced graphene oxide (rGO) was coated on the AgNWs to enhance the adhesion between NWs, by forming a PDMS sandwich structure [7,20]. By using PUU dispersed with ZnS microparticles onto the AgNWs/PDMS film, Kim et al. could fabricate electroluminescent (EL) devices, which could be stretched up to 150% and survived 5000 cycles of 100% applied strain, as shown in Figure 1c. This may be due to the overcoating of PUU on the AgNWs deposited on the hydroxylated PDMS that resulted in a superstable, stretchable transparent electrode, in which the hydrogen bonding between the hydroxyl groups and urea (or urethane) potentially enhances the interlayer interactions. Similarly, the AgNW/rGO electrodes embedded into a PU dielectric layer showed no significant change in resistance

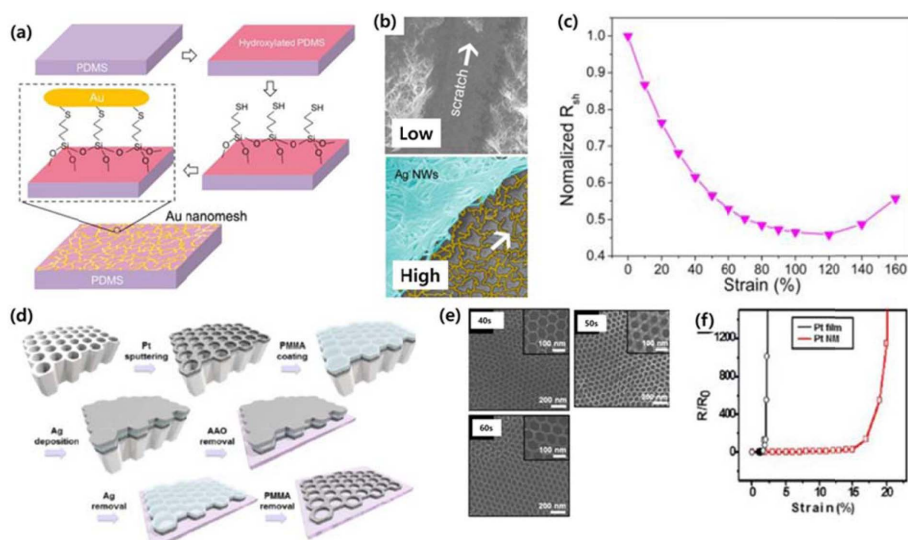


Figure 2(a) Schematic of the formation of chemical bonds between the AuNM and the underlying PDMS. (b) Low and high-magnification SEM images of a S-AuNM with a AgNW network on top scratched by tweezers and micropipette tip, respectively. (c) Normalized sheet resistance of a SAuNM with a 100% pre-strain as a function of tensile strain. (a), (b) and (c) Reprinted with permission from [24], Z. F. Ren et al., *Nano letters* 16, 1 (2016). © 2017, American Chemical Society. (d) Schematic representation of synthesis of Pt nanomesh structure. (e) SEM images of Pt nanomesh structure films with various bridge widths in sputtering time of 40 s, 50 s, and 60 s. (f) Change in resistance (R/R_0 , where R_0 is the initial resistance at zero strain) of Pt film and nanomesh structure film transferred on PDMS substrate stretched toward the xy plane by ~25%. (d), (e) and (f) Reprinted with permission from [31], S. Park et al., *Chem Mater* 25, 16 (2013). © 2017, American Chemical Society.

under 50% of strain, as shown in Figure 1d. The addition of rGO on AgNWs enhanced both the conductance and stretchability of the AgNW conducting network. The different Poisson's ratios between the PDMS substrate and PU dielectric layer helped to reduce the stretch strain at the junctions of NWs.

2. Nanostructured networks

As mentioned above, there are several issues associated with the fabrication of stretchable transparent electrodes by using AgNWs, such as the difficulty in achieving a homogeneous dispersion of the nanowires, haze effect caused by irregular NW arrays making the electrode opaque, and poor adhesion between the NWs and the substrate. Thus, several bottom-up strategies to fabricate nanostructured networks by using metal deposition have also been reported [24,27,30-31].

Figure 2a shows the fabrication method of a prestrained Au nanomesh (AuNM) stretchable transparent electrode. In order to improve the adhesion between the AuNMs and the PDMS substrate, Ren et al. employed 3-mercaptopropyltrimethoxysilane (MPTMS) molecules to form Au-S bonds. After producing hydroxyl groups (oxidation) on PDMS, the MPTMS molecules can form a self-assembled monolayer (SAM) on it through the formation of chemical bonds (-Si-O-Si- units). The deposition of Au on the assembled MPTMS SAM surface was then obtained by using grain boundary lithography, which uses the open grain boundary network of a SAM structure as deposition site. Figure 2b shows the low and high-magnification SEM images of an S-AuNM covered

by an AgNW network, upon scratching by tweezers, indicating that the S-AuNM still remains on the substrate, while the Ag NWs are mostly removed. The S-AuNMs exhibited a much better scratch-resistance than the solution-processed AgNW networks. As it can be observed in Figure 2b, the S-AuNM exhibits an enhanced adhesion on the PDMS substrate compared with AgNW. Furthermore, the firmly adhered S-AuNM retained its original morphology even after the scratch-test. The normalized sheet resistance change of the prestrained S-AuNM is shown in Figure 2c. The sheet resistance of the prestrained S-AuNM decreased until 120% of the strain, while the normalized sheet resistance was less than 0.5 in the range from 70 to 140% of stretch strain.

Unlike grain boundary lithography that produces irregular nanostructures, Park et al. fabricated metallic nanomesh architectures by using anodized aluminum oxide (AAO) templates and metal sputtering. The synthetic routes to produce stretchable transparent metallic nanomeshes are illustrated in Figure 2d. Particularly, AAO templates have large, ordered, and tunable dimensions; moreover, their pore size and periodicity can be easily modulated. After sputtering of Pt on one side of an AAO template, a PMMA adlayer is formed on the top of Pt, followed by the deposition of Ag on top of PMMA. The final Pt nanomesh, whose structure is a replica of the AAO, is then fabricated by sequential removal of the AAO, Ag, and PMMA and transfer onto a PDMS substrate. Figure 2e shows the SEM images of Pt nanomesh structure films formed with a sputtering time of 40, 50, and 60 s. The resulting nanomeshes exhibited a bridge width of 11 ± 2 ,

22 ± 3 , and 30 ± 2 nm, respectively, upon increasing of the sputtering time. Therefore, by using an AAO template and metal sputtering, it was found that the sheet resistance and transmittance of stretchable transparent electrodes could be easily modulated by adjusting the sputtering time. The change in resistance of the Pt film (R/R_0 , where R_0 is the initial resistance at zero strain) with a nanomesh structure film transferred on a PDMS substrate is shown in Figure 2f. It can be seen that the Pt film is a bulk type film that has a thickness of 22 nm without exhibiting any nanomesh pattern. The Pt film and Pt NM were stretched in the y-axis direction. In the case of the Pt film, no resistance change ensued up to a 2.0% stretch ratio; however, an electrical disconnection suddenly occurred at 2.3% stretch strain as indicated by a dramatic increase in resistance. On the other hand, PtNM retained its initial resistance up to 16.8% stretch ratio, but finally also lost its conductivity under a further stretch strain. In conclusion, PtNM possessed a 7 times higher mechanical tolerance than the bulk Pt film. Furthermore, the presented metal architecture is easy to scale up and can be fabricated using various metals, thus it is expected that similar noble metal architectures may exhibit a localized surface plasmon effect.

3. Conductive polymers

The above-mentioned stretchable transparent electrodes composed of metallic nanomaterials should be fabricated in such a manner that a vacant space is formed between the electrodes in order to allow the light to pass through. Conductive polymers, which are represented by poly(3,4-ethylenedioxythiophene) doped with poly(styrenesulfonate) (PEDOT:PSS) and pyrolyzed polydopamine (PPD), are also promising candidate materials because of their high transparency, excellent film uniformity, high conductivity, and ability to reversibly withstand mechanical deformations. The electrical conductivity of conductive polymers can be improved by increasing their film thickness; however, this leads to a reduced transparency due to their characteristic absorption of the light in the visible wavelength region. Therefore, different efforts have been concentrated to improve the properties of conductive polymers and utilize them for the fabrication of stretchable transparent electrodes [32-36].

Bao et al. found that highly conductive and transparent PEDOT:PSS films could be obtained with the use of the fluorosurfactant Zonyl as additive [35]. In order to obtain a PEDOT:PSS solution, 5 wt% of dimethylsulfoxide (DMSO) and different amounts of Zonyl were added to PEDOT:PSS. DMSO is a 'secondary dopant', which improves the morphology and conductivity of PEDOT:PSS films by 2 to 3 orders of magnitude. Figure 3 shows the direct current (DC) to optical conductivity ratio and sheet resistance as a function of the Zonyl concentration in wt%. Bao et al. found that the use of Zonyl, in addition to DMSO, enhanced the conductivity of PEDOT:PSS. The

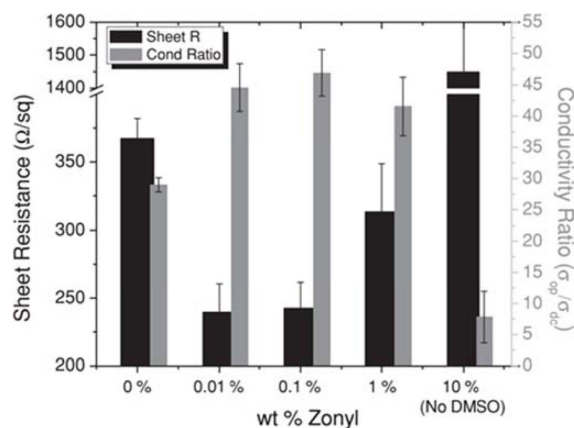


Figure 3. DC to optical conductivity ratios (σ_{dc}/σ_{opt}) and sheet resistance (R_s) vs Zonyl concentration in wt% for four samples per condition across two batches. Reprinted with permission from [24], Z. A. Bao et al., *Adv Funct Mater* 22, 2 (2012). © 2017, John Wiley & Sons, Inc.

sheet resistance of the PEDOT:PSS without any additives was over $105 \Omega^{-1}$ at 97% of transparency (at 550 nm). With the addition of 5 wt% DMSO, the sheet resistance decreased to $370 \Omega^{-1}$ at 97% Tr (transmittance). However, as the amount of Zonyl increased from 0.01 to 0.1 wt%, the conductivity further increased by 35% to $240 \Omega^{-1}$ with no transmittance change at 550 nm for one-layer films.

Another issue that has been raised is the achievement of stretchability, while maintaining or improving conductivity. Conductive polymers possess an excellent electrical conductivity and mechanical stability during the 'stretch and restore' process; however, their conductivity decreases when a strain force is applied. In order to improve the stretchability of conductive polymers, many researchers have explored the formation of composite structures between conductive polymers and other support materials. Lee et al. functionalized PEDOT:PSS with ionic liquids to enhance its mechanical properties, and achieved an improved stretchability upon application of a longitudinal stretching strain [32]. The authors selected 1-ethyl-3-methylimidazolium tetracyanoborate (EMIM TCB) as ionic liquid, which was added to an aqueous PEDOT:PSS solution in amounts ranging from 0.5 to 1.0 wt%, and observed the corresponding changes in conductivity and sheet resistance, as shown in Figure 4a and 4b, respectively. By increasing the concentration of EMIM TCB, the conductivity continuously increased from 1 S cm^{-1} for pristine PEDOT:PSS to 1280 S cm^{-1} for 1.5 wt% EMIM TCB containing PEDOT:PSS. Although highly concentrated PEDOT:PSS solutions containing EMIM TCB exhibited a higher conductivity of the composite films, the >2.0 wt% EMIM TCB solutions were too viscous to be solution-processed and also partly precipitated owing to aggregation. Therefore, the PEDOT:PSS containing below 1.5 wt% EMIM TCB displayed a better uniformity and smooth surface roughness of the films. Figure 4b shows the change in normalized resistance (i.e., $R/R_0 = \text{final}$

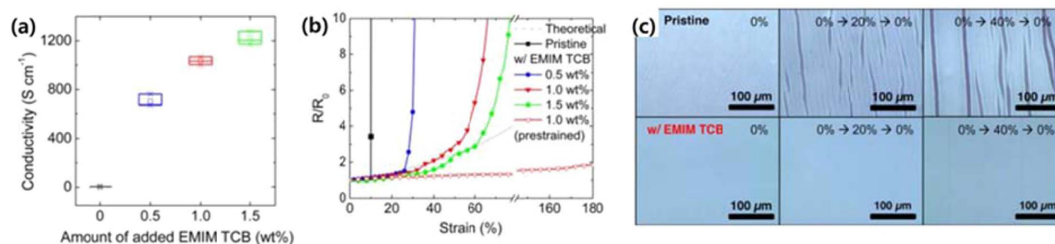


Figure 4(a). Conductivities of PEDOT:PSS films with various concentrations of EMIM TCB. **(b)** Normalized resistances of PEDOT:PSS films with various concentrations of EMIM TCB when PDMS substrates were stretched from 0% to 180%. **(c)** Optical microscope images of PEDOT:PSS films with and without 1.0 wt % EMIM TCB after stretching and releasing with various strains. Reprinted with permission from [32], K. Lee et al., *ACS Appl Mater Inter* 9, 1 (2017). © 2017, American Chemical Society.

resistance/initial resistance) as a function of the tensile strain (ε) for the film containing EMIM TCB at various densities. Figure 4c illustrates the optical microscopic images of the PEDOT:PSS films with and without 1.0 wt% EMIM TCB after stretching and releasing under various stretching strains. The pristine film was broken under strains as low as 10%. In contrast, the PEDOT:PSS films blended with amounts of EMIM TCB ranging from 0.5 to 1.5 wt% exhibited a gradual increase of strain-stability.

4. Carbon-based electrodes

Carbon-based electrodes, including carbon nanotubes (CNTs) and graphene, are alternative transparent electrodes endowed with a high transparency and flexibility, although they possess a relatively low electrical conductivity. Therefore, many research groups have attempted to increase the electrical conductivity of these electrodes by using chemical treatments or forming hybrid structures with other conductive and transparent materials [37-44].

CNTs are the earliest developed carbon-based materials that have been actively investigated to increase the physical elasticity and mechanical strength by combination with various steel materials. Since the discovery of the physical flexibility and high transparency of CNTs, various studies have been conducted to establish them as substitutes for next generation transparent and stretchable electrodes. In order to overcome the drawbacks of CNTs mentioned above, Zhou et al. enhanced their electrical conductivity by sequential treatment with nitric acid and chloroauric acid (HAuCl₄), thus forming Au-CNTs [37]. The initial value of sheet resistance of the CNT film treated with nitric acid was 182 Ω^{-1} . The sheet resistance decreased to 92 Ω^{-1} after immersion in nitric acid. In order to enhance the conductivity of the CNT film further, a solution of chloroauric acid in ethanol was spin coated on the CNT film. As the concentration of HAuCl₄ increased, the sheet resistance of the CNT film decreased significantly owing to the large reduction potential of the Au³⁺ ion, which is a p-type dopant and thus aids to increase the conductivity of the CNT film. Moreover, the sheet resistance of the Au-CNT film decreased rapidly at 5 mM, and remained steadily low at higher concentrations.

Graphene is a well-known new generation carbon-based material that is most commonly studied as a transparent electrode, after Geim revealed its excellent electrical and physical properties [45-49]. However, in view of its use as a stretchable electrode, its stretchability is limited by the high stiffness of graphene in two dimensions. Thus, recent research on stretchable graphene electrodes has been carried out concerning the structure design or its combination with other materials [38,43-44].

Park et al. reported a fabrication method of omnidirectionally stretchable and transparent graphene electrodes [39]. Figure 5a shows the schematic illustration of the step-by-step fabrication method of a transparent and stretchable graphene electrode including PDMS spin-coating, curing, and Cu etching processes. In order to enhance the stretchability of graphene, Cu foil was prepatterned by pressing it with a Fresnel lens, which acted as a patterning mold. Then, after the growth of graphene, PDMS was spin-coated on the prepatterned Cu foil. As final step, the PDMS film was thermally cured, and the Cu foil was chemically etched by using a Cu etchant. Figure 5b shows the photograph of a graphene/PDMS free-standing film, which exhibited well-defined, concentric circle patterns. The mechanically enhanced flexible and stretchable properties of textured graphene compared with flat graphene are depicted in Figure 5c and 5d. When the film was folded with a bending radius (r) as small as $r = 0.5$ mm and stretched up to 30% of the tensile stress, the textured graphene/PDMS film maintained its electrical properties. Furthermore, the recovered sheet resistance of the textured graphene/PDMS film was nearly the same under both bending and stretching conditions.

Park et al. combined graphene with a metal nanowire or metal nanotrough to produce hybrid structures for high performance and stretchable electrodes [43-44]. Compared to a single graphene sheet, metal nanowire, or metal nanotrough, the formation of a hybrid structure can improve the mechanical stiffness against the stretching strain due to the percolating network, which simultaneously charge transport in the hybrid nanostructure. Figures 6a-c show the SEM images and the change of sheet resistance of each hybrid graphene/metal nanowire and graphene/metal

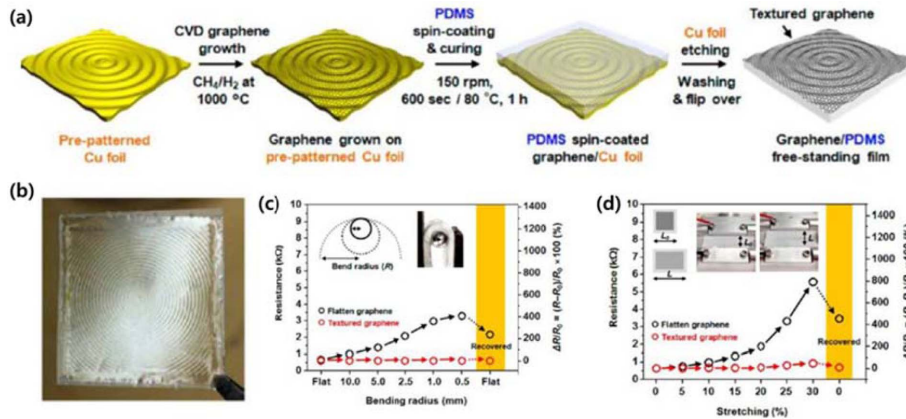


Figure 5(a). Schematic illustration of the different steps in the fabrication of transparent conductive electrodes including CVD graphene growth, PDMS spin-coating, curing, and Cu etching. (b) Photograph of a graphene/PDMS free-standing film. (c) and (d) Variation in resistance of a textured graphene/PDMS film as a function of bending radius and tensile strains (insets: actual test images for a graphene/PDMS film). Reprinted with permission from [39], H. S. Park et al., *ACS Nano* 10, 10 (2016). © 2017, American Chemical Society.

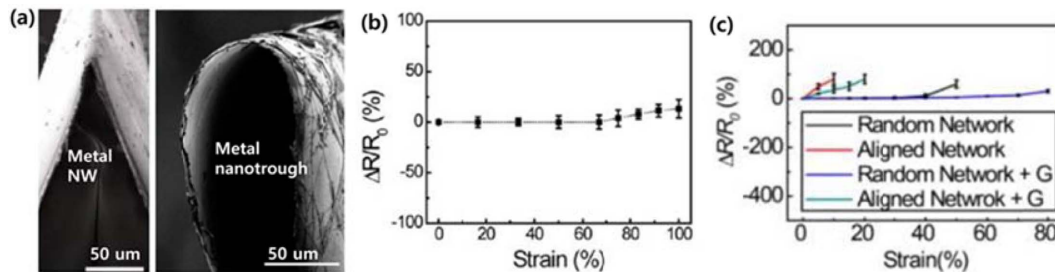


Figure 6(a). SEM image of the hybrid electrode folded in half. (b) Relative difference in resistance as a function of radius of curvature. (c) Relative resistance changes of the nanotrough or the hybrid as a function of strain. Reprinted with permission from [43,44], J. U. Park et al., *Nano Letters* 14, 11 (2014) and *Nano Letters* 13, 6 (2013). © 2017, American Chemical Society.

nanotrough, respectively. As it can be seen in Figure 6b, the hybrid graphene/metal nanowire electrode could be stretched up to 100% tensile strain with a negligible resistance change. Moreover, it was found that a randomly arrayed nanotrough with graphene could further enhance the stretchability compared to an aligned nanotrough network with graphene, as shown in Figure 6c. These results show that the combination of graphene with a metal nanowire or metal nanotrough improves the stretchability since the graphene layer can maintain its conductive paths by covering the local disconnections of the metal lines.

III. Conclusions

Stretchable and transparent electrodes are one of the most important components in wearable electronics. Herein, recent advances in the development of stretchable and transparent electrodes using AgNWs, nanostructured networks, conductive polymers, and carbon-based electrodes have been discussed. Especially, the fabrication methods and characterization of stretchable and transparent electrodes have been described in detail in this review. Although various approaches have been explored so far to enhance the stretchability while maintaining the transparency, there are still requirements that need to be met. Each type of

stretchable and transparent electrode has some inherent problems, and various strategies to solve these aspects are required. In the case of AgNWs, remaining issues are related to the dispersion of the NWs and the haze effect. The nanostructured electrodes possess a relatively low stretchability, while the electrical conductivity of conductive polymers and carbon-based materials should be enhanced to be used as conductors.

Over the past decade, tremendous research efforts have revealed that the development of stretchable and transparent electrodes is one of the most important engineering platforms to realize wearable electronics. Applications employing new generation stretchable electronics, including bioelectronics, biomedical, healthcare, and wearable devices, are expected to emerge and change our life in the near future.

Reference and Notes

- [1] Y. Huang, L. Gao, Y. N. Zhao, X. H. Guo, C. X. Liu, and P. Liu, Highly flexible fabric strain sensor based on graphene nanoplatelet-polyaniline nanocomposites for human gesture recognition. *J Appl Polym Sci* 2017, 134(39).
- [2] B. G. Zhuo, S. J. Chen, M. M. Zhao, and X. J. Guo, High Sensitivity Flexible Capacitive Pressure Sensor Using Polydimethylsiloxane Elastomer Dielectric Layer Micro-Structured by 3-D Printed Mold. *Ieee J Electron Devi* 2017, 5(3), 219-223.

- [3] Y. C. Zhao and X. Huang, Mechanisms and Materials of Flexible and Stretchable Skin Sensors. *Micromachines-Basel* 2017, 8(3).
- [4] X. Q. Zhang, X. X. Huang, L. Xia, B. Zhong, X. D. Zhang, T. Zhang, and G. W. Wen, Facile synthesis of flexible and free-standing cotton covered by graphene/MoO₂ for lithium-ions batteries. *Ceram Int* 2017, 43(6), 4753-4760.
- [5] P. Zhang, H. Z. Zhang, C. Yan, Z. J. Zheng, and Y. Yu, Highly conductive templated-graphene fabrics for lightweight, flexible and foldable supercapacitors. *Mater Res Express* 2017, 4(7).
- [6] X. G. Yu, Y. Q. Li, W. B. Zhu, P. Huang, T. T. Wang, N. Hu, and S. Y. Fu, A wearable strain sensor based on a carbonized nano-sponge/silicone composite for human motion detection. *Nanoscale* 2017, 9(20), 6680-6685.
- [7] B. You, Y. Kim, B. K. Ju, and J. W. Kim, Highly Stretchable and Waterproof Electroluminescence Device Based on Superstable Stretchable Transparent Electrode. *Acs Appl Mater Inter* 2017, 9(6), 5486-5494.
- [8] K. Kim, J. Kim, B. G. Hyun, S. Ji, S. Y. Kim, S. Kim, B. W. An, and J. U. Park, Stretchable and transparent electrodes based on in-plane structures. *Nanoscale* 2015, 7(35), 14577-14594.
- [9] K. Kim, B. G. Hyun, J. Jang, E. Cho, Y. G. Park, and J. U. Park, Nanomaterial-based stretchable and transparent electrodes. *J Inf Disp* 2016, 17(4), 131-141.
- [10] S. Jang, W. B. Jung, C. Kim, P. Won, S. G. Lee, K. M. Cho, M. L. Jin, C. J. An, H. J. Jeon, S. H. Ko, T. S. Kim, and H. T. Jung, A three-dimensional metal grid mesh as a practical alternative to ITO. *Nanoscale* 2016, 8(29), 14257-14263.
- [11] T. Bocksrocker, N. Hulsmann, C. Eschenbaum, A. Pargner, S. Hofle, F. Maier-Flaig, and U. Lemmer, Highly efficient fully flexible indium tin oxide free organic light emitting diodes fabricated directly on barrier-foil. *Thin Solid Films* 2013, 542, 306-309.
- [12] J. S. Oh, J. S. Oh, J. H. Shin, G. Y. Yeom, and K. N. Kim, Nano-Welding of Ag Nanowires Using Rapid Thermal Annealing for Transparent Conductive Films. *J Nanosci Nanotechnol* 2015, 15(11), 8647-8651.
- [13] H. T. Zhai, R. R. Wang, X. Wang, Y. Cheng, L. J. Shi, and J. Sun, Transparent heaters based on highly stable Cu nanowire films. *Nano Res* 2016, 9(12), 3924-3936.
- [14] X. M. Xu, S. He, C. H. Zhou, X. D. Xia, L. Xu, H. Chen, B. C. Yang, and J. L. Yang, Largely-increased length of silver nanowires by controlled oxidative etching processes in solvothermal reaction and the application in highly transparent and conductive networks. *Rsc Adv* 2016, 6(107), 105895-105902.
- [15] M. X. Song, X. He, C. Z. Zhang, M. D. Chen, C. J. Huang, F. H. Chen, and H. Qiu, Solvothermal fabrication of thin Ag nanowires assisted with AAO. *Rsc Adv* 2016, 6(85), 82238-82243.
- [16] S. Pirsalami, S. M. Zebarjad, and H. Daneshmanesh, An Overview of Metallic Nanowire Networks, Promising Building Blocks for Next Generation Transparent Conductors: Emergence, Fundamentals and Challenges. *J Electron Mater* 2017, 46(8), 4707-4715.
- [17] J. T. Jiu and K. Sugauma, Metallic Nanowires and Their Application. *Ieee T Comp Pack Man* 2016, 6(12), 1733-1751.
- [18] Y. Kim, S. Jun, B. K. Ju, and J. W. Kim, Heterogeneous Configuration of a Ag Nanowire/Polymer Composite Structure for Selectively Stretchable Transparent Electrodes. *Acs Appl Mater Inter* 2017, 9(8), 7505-7514.
- [19] D. H. Kim, K. C. Yu, Y. Kim, and J. W. Kim, Highly Stretchable and Mechanically Stable Transparent Electrode Based on Composite of Silver Nanowires and Polyurethane-Urea. *Acs Appl Mater Inter* 2015, 7(28), 15214-15222.
- [20] T. Y. Choi, B. U. Hwang, B. Y. Kim, T. Q. Trung, Y. H. Nam, D. N. Kim, K. Eom, and N. E. Lee, Stretchable, Transparent, and Stretch-Unresponsive Capacitive Touch Sensor Array with Selectively Patterned Silver Nanowires/Reduced Graphene Oxide Electrodes. *Acs Appl Mater Inter* 2017, 9(21), 18022-18030.
- [21] H. S. Liu, B. C. Pan, and G. S. Liou, Highly transparent AgNW/PDMS stretchable electrodes for elastomeric electrochromic devices. *Nanoscale* 2017, 9(7), 2633-2639.
- [22] C. Hwang, J. An, B. D. Choi, K. Kim, S. W. Jung, K. J. Baeg, M. G. Kim, K. M. Ok, and J. Hong, Controlled aqueous synthesis of ultra-long copper nanowires for stretchable transparent conducting electrode. *J Mater Chem C* 2016, 4(7), 1441-1447.
- [23] G. Heo, K. H. Pyo, D. H. Lee, Y. Kim, and J. W. Kim, Critical Role of Diels-Adler Adducts to Realise Stretchable Transparent Electrodes Based on Silver Nanowires and Silicone Elastomer. *Sci Rep-Uk* 2016, 6.
- [24] C. F. Guo, Y. Chen, L. Tang, F. Wang, and Z. F. Ren, Enhancing the Scratch Resistance by Introducing Chemical Bonding in Highly Stretchable and Transparent Electrodes. *Nano Letters* 2016, 16(1), 594-600.
- [25] T. Araki, R. Mandamparambil, D. M. P. van Bragt, J. Jiu, H. Koga, J. van den Brand, T. Sekitani, den J. M. J. Toonder, and K. Sugauma, Stretchable and transparent electrodes based on patterned silver nanowires by laser-induced forward transfer for non-contact printing techniques. *Nanotechnology* 2016, 27(45).
- [26] J. B. Pyo, B. S. Kim, H. Park, T. A. Kim, C. M. Koo, J. Lee, J. G. Son, S. S. Lee, and J. H. Park, Floating compression of Ag nanowire networks for effective strain release of stretchable transparent electrodes. *Nanoscale* 2015, 7(39), 16434-16441.
- [27] C. F. Guo, T. Y. Sun, Q. H. Liu, Z. G. Suo, and Z. F. Ren, Highly stretchable and transparent nanomesh electrodes made by grain boundary lithography. *Nat Commun* 2014, 5.
- [28] T. Cheng, Y. Z. Zhang, W. Y. Lai, Y. Chen, W. J. Zeng, and W. Huang, High-performance stretchable transparent electrodes based on silver nanowires synthesized via an eco-friendly halogen-free method. *J Mater Chem C* 2014, 2(48), 10369-10376.
- [29] W. L. Hu, X. F. Niu, L. Li, S. R. Yun, Z. B. Yu, and Q. B. Pei, Intrinsically stretchable transparent electrodes based on silver-nanowire-crosslinked-polyacrylate composites. *Nanotechnology* 2012, 23(34).
- [30] H. Yabu, K. Nagamine, J. Kamei, Y. Saito, T. Okabe, T. Shimazaki, and M. Nishizawa, Stretchable, transparent and molecular permeable honeycomb electrodes and their hydrogel hybrids prepared by the breath figure method and sputtering of metals. *Rsc Adv* 2015, 5(107), 88414-88418.
- [31] H. Y. Jang, S. K. Lee, S. H. Cho, J. H. Ahn, and S. Park, Fabrication of Metallic Nanomesh: Pt Nano-Mesh as a Proof of Concept for Stretchable and Transparent Electrodes. *Chem Mater* 2013, 25(17), 3535-3538.
- [32] M. Y. Teo, N. Kim, S. Kee, B. S. Kim, G. Kim, S. Hong, S. Jung, and K. Lee, Highly Stretchable and Highly Conductive PEDOT:PSS/Ionic Liquid Composite Transparent Electrodes for Solution-Processed Stretchable Electronics. *Acs Appl Mater Inter* 2017, 9(1), 819-826.
- [33] J. G. Tait, B. J. Worfolk, S. A. Maloney, T. C. Hauger, A. L. Elias, J. M. Buriak, and K. D. Harris, Spray coated high-conductivity PEDOT:PSS transparent electrodes for stretchable and mechanically-robust organic solar cells. *Sol Energ Mat Sol C* 2013, 110, 98-106.
- [34] R. J. Li, K. Parvez, F. Hinkel, X. L. Feng, and K. Mullen, Bioinspired Wafer-Scale Production of Highly Stretchable Carbon Films for Transparent Conductive Electrodes. *Angew Chem Int Edit* 2013, 52(21), 5535-5538.
- [35] M. Vosgueritchian, D. J. Lipomi, and Z. A. Bao, Highly Conductive and Transparent PEDOT:PSS Films with a Fluorosurfactant for Stretchable and Flexible Transparent Electrodes. *Adv Funct Mater* 2012, 22(2), 421-428.
- [36] Y. G. Seol, T. Q. Trung, O. J. Yoon, I. Y. Sohn, and N. E. Lee, Nanocomposites of reduced graphene oxide nanosheets and conducting polymer for stretchable transparent conducting electrodes. *J Mater Chem* 2012, 22(45), 23759-23766.
- [37] Q. X. Fan, Q. Zhang, W. B. Zhou, F. Yang, N. Zhang, S. Q. Xiao, X. G. Gu, Z. J. Xiao, H. L. Chen, Y. C. Wang, H. P. Liu, and W. Y. Zhou, Highly conductive and transparent carbon nanotube-based electrodes for ultrathin and stretchable organic solar cells. *Chinese Phys B* 2017, 26(2).
- [38] J. H. Liu, Y. H. Yi, Y. H. Zhou, and H. F. Cai, Highly Stretchable and Flexible Graphene/ITO Hybrid Transparent Electrode. *Nanoscale Res Lett* 2016, 11.
- [39] J. Y. Hong, W. Kim, D. Cho, J. Kong, and H. S. Park, Omnidirectionally Stretchable and Transparent Graphene Electrodes. *Acs Nano* 2016, 10(10), 9446-9455.
- [40] S. Ahn, A. Choe, J. Park, H. Kim, J. G. Son, S. S. Lee, M. Park, and H. Ko, Directed self-assembly of rhombic carbon nanotube nanomesh films for transparent and stretchable electrodes. *J Mater Chem C* 2015, 3(10), 2319-2325.
- [41] S. Won, Y. Hwangbo, S. K. Lee, K. S. Kim, K. S. Kim, S. M. Lee, H. J. Lee, J. H. Ahn, J. H. Kim, and S. B. Lee, Double-layer CVD graphene as stretchable transparent electrodes. *Nanoscale* 2014, 6

- (11), 6057-6064.
- [42] T. Chen, Y. H. Xue, A. K. Roy, and L. M. Dai, Transparent and Stretchable High-Performance Supercapacitors Based on Wrinkled Graphene Electrodes. *Acs Nano* 2014, 8(1), 1039-1046.
- [43] B. W. An, B. G. Hyun, S. Y. Kim, M. Kim, M. S. Lee, K. Lee, J. B. Koo, H. Y. Chu, B. S. Bae, and J. U. Park, Stretchable and Transparent Electrodes using Hybrid Structures of Graphene-Metal Nanotrough Networks with High Performances and Ultimate Uniformity. *Nano Letters* 2014, 14(11), 6322-6328.
- [44] M. S. Lee, K. Lee, S. Y. Kim, H. Lee, J. Park, K. H. Choi, H. K. Kim, D. G. Kim, D. Y. Lee, S. Nam, and J. U. Park, High-Performance, Transparent, and Stretchable Electrodes Using Graphene-Metal Nanowire Hybrid Structures. *Nano Letters* 2013, 13(6), 2814-2821.
- [45] K. S. Novoselov, A. K. Geim, S. V. Morozov, D. Jiang, Y. Zhang, S. V. Dubonos, I. V. Grigorieva, and A. A. Firsov, Electric field effect in atomically thin carbon films. *Science* 2004, 306(5696), 666-669.
- [46] A. K. Geim and K. S. Novoselov, The rise of graphene. *Nature materials* 2007, 6(3), 183-191.
- [47] A. A. Balandin, S. Ghosh, W. Bao, I. Calizo, D. Teweldebrhan, F. Miao, and C. N. Lau, Superior thermal conductivity of single-layer graphene. *Nano letters* 2008, 8(3), 902-907.
- [48] X. Li, G. Zhang, X. Bai, X. Sun, X. Wang, E. Wang, and H. Dai, Highly conducting graphene sheets and Langmuir-Blodgett films. *Nat Nanotechnol* 2008, 3(9), 538-542.
- [49] M. D. Stoller, S. Park, Y. Zhu, J. An, and R. S. Ruoff, Graphene-based ultracapacitors. *Nano letters* 2008, 8(10), 3498-3502.